

Two-dimensional Weyl materials in the presence of constant magnetic fields

Yaraslau Tamashevich¹, Leone Di Mauro Villari² and Marco Ornigotti¹

¹*Faculty of Engineering and Natural Sciences, Tampere University, Tampere 33720, Finland*

²*Department of Physics and Astronomy, University of Manchester, Manchester M13 9PL, United Kingdom*



(Received 9 September 2022; revised 4 May 2023; accepted 14 June 2023; published 26 June 2023)

In this work we investigate the effect of a constant external, or artificial, magnetic field on the nonlinear response of two-dimensional (2D) Weyl materials. We calculate the Landau levels for tilted cones in 2D Weyl materials by treating the tilting in a perturbative manner and employ perturbation theory to calculate the tilting-induced correction to the magnetic field induced Landau spectrum. We then calculate the induced current as a function of the tilting coefficients and extract the corresponding nonlinear signal. Then, we analyze how changing the tilting parameter affects the nonlinear signal. Our findings show the possibility of achieving a significant tunability of the nonlinear response by suitably engineering the orientation and degree of tilt of Dirac cones in 2D Weyl materials.

DOI: [10.1103/PhysRevB.107.245425](https://doi.org/10.1103/PhysRevB.107.245425)

I. INTRODUCTION

In the last 18 years, after the discovery of graphene [1,2], the study of two-dimensional pseudorelativistic fermions has dominated the condensed matter arena. The study of graphene in a uniform magnetic field also contributed to this boom with the discovery of the anomalous, *half-integer* quantum Hall effect [3]. The basic theory stems from the quantization of cyclotron orbits in a uniform magnetic field, the Landau quantization (LQ). The carriers can occupy only orbits with discrete, equidistant energy values, called Landau levels (LLs) [4]. LQ plays an important role in the electronic properties of materials. It is directly responsible for diamagnetism and, at strong magnetic field, leads to oscillation of the magnetic susceptibility and conductivity, known as the de Haas–Van Alphen [5] and Shubnikov–de Haas [6,7] effects, respectively.

Over the past decade, several theoretical and experimental works dealt with the problem of characterizing the behavior of Weyl semimetals in the presence of magnetic fields, including describing the effect of tilting on the LL spectrum both semiclassically [8] and with a full relativistic quantum treatment [9]. These results have been applied to characterize the effect of the tilt on LL spectroscopy and revealed salient features of the evolution of the absorption spectrum of two-dimensional (2D) Dirac fermions upon tilt, such as the insurgence of nondipolar transitions as a consequence of the tilt [10,11]. The effect of tilting on LLs has also been studied in three-dimensional Weyl materials, for which similar results have been found [12].

Despite the great interest this topic has attracted, especially for 2D materials, no study on the simultaneous effect of cone tilting and LLs on the nonlinear optical response of such materials has been carried out, to the best of our knowledge. For this reason, in this paper we focus our attention on LLs of tilted, type-II Weyl materials (WMs). Type-II WMs were first postulated in 2015 [13]. In contrast to type-I WMs, which have straight cones at the nodal point and preserve Lorentz invariance, they are tilted and have broken Lorentz

invariance. Type-II cones typically occur when type-I Weyl nodes are tilted enough, along some specific direction, that a Lifshitz transition occurs and the system acquires a finite density of states at the Weyl node. Type-II fermions, either Dirac or Weyl, have been found in a variety of materials such as semimetals, transition metal dichalcogenides (PtTe₂, WTe₂) [14], LaAlO₃/LaNiO₃/LaAlO₃ quantum wells [15], and PdTe₂ superconductors [16]. The electronic properties of these materials have been extensively studied in the last few years [17–20]. The nonlinear optics has also recently started to attract some attention [21–23].

In this work we focus on two-dimensional materials with type-II Weyl fermions (WFs), which have been theoretically explored with increasing attention in the last few years [24–29]. Although a conclusive experimental observation is still lacking, they are not unrealistic. In fact, a promising platform for the experimental realization of such materials is, for example, the organic compound α -(BEDT-TTF)₂I₃, a quasi-2D conductor which supports WFs [30–32]. In particular, we study the nonlinear optical response of the Landau levels in type-II WMs. Although a fully relativistic and non-perturbative approach, following Ref. [9], could be employed to calculate the effect of the tilting on LLs, we instead opt for a perturbative approach, which allows us to write a set of coupled mode equations for the time-dependent population coefficients and calculate the induced current as a function of such coefficients and the corresponding nonlinear spectrum directly in the laboratory frame, rather than in the boosted frame. This allows for a more direct and experiment-friendly approach to the problem. Notice, however, that treating the tilting perturbatively does not compromise the nature of the Dirac cones or, ultimately, the nature of the considered material. However, to avoid confusion between a proper type-II material, defined by the touching point of the electron and hole pockets, and the perturbative type-II material discussed in this work, we will refer to our system as quasi-type-II.

Our results clearly show how it is possible to control and enhance the nonlinear response of 2D Weyl materials using an

external, or artificial (generated, for example, through bending or strain [33]), magnetic field. We, in fact, show how a suitable combination of magnetic field control and material engineering, in the form of control of the degree of tilt of Dirac cones, can lead to efficient generation of high harmonics, up to order 50 and beyond. This could lead to significant applications in optics and photonics. The possibility to control the nonlinear optical response of such materials by controlling both the applied magnetic field and the degree of tilt of Dirac cones in such materials, in fact, could lead to reconfigurable, broadband, efficient frequency converters. On the other hand, the same device could also be used for sensing applications, essentially exploiting the fact that external perturbation either can change the local crystalline structure of Weyl materials (thus amounting to an overall change in the intensity of the applied magnetic field, for example) or can induce anisotropies, which could change the degree of tilting, thus allowing the use of the intrinsic anisotropic nature of the nonlinear optical response of 2D Weyl materials [23]. In both cases, analyzing the effects of such perturbations on the nonlinear optical response of 2D Weyl materials might prove insightful for sensing applications.

This paper is organized as follows: In Sec. II we introduce the Hamiltonian for tilted two-dimensional Weyl materials in the presence of an external gauge field. In Sec. III we compute the tilt-induced perturbation on Landau levels. In Secs. IV and V we focus on the nonlinear optical response by considering the interaction of the Landau level with the impinging electric field. Finally, conclusions are drawn in Sec. VI.

II. TILTED HAMILTONIAN FOR 2D WEYL MATERIALS

The Hamiltonian for a 2D Weyl material in the presence of an external electromagnetic field [described by the vector potential $\mathbf{A}(t)$] and a gauge field [described by the U(1) gauge potential $\mathbf{A}^{(g)}$] is given by

$$\hat{H} = \sum_{i=1}^2 v_i p_i \hat{\sigma}_i + \Delta \hat{\sigma}_3 + \mathbf{a} \cdot \mathbf{p} \hat{\sigma}_0, \quad (1)$$

where $\hat{\sigma}_k$ are Pauli matrices (with $\hat{\sigma}_0 = \mathbb{I}$ being the two-dimensional identity matrix); $\mathbf{a} = (a_x, a_y)$ is the tilting vector; $v_{x,y}$ are the (anisotropic) Fermi velocities along the x and y directions, respectively; Δ is a staggered potential, which accounts for the gap between the valence and conduction bands; and \mathbf{p} is the minimally coupled kinetic momentum, which takes into account both the impinging electromagnetic field and the external (or artificial) magnetic field, i.e.,

$$p_\mu = k_\mu + \frac{e}{c} A_\mu^{(g)} + \frac{e}{c} A_\mu, \quad (2)$$

where $k_{x,y}$ are the Cartesian components of the momentum. For later convenience, we also define the minimally coupled magnetic momentum $\pi_\mu = k_\mu + \frac{e}{c} A_\mu^{(g)}$, which will be useful in constructing the unperturbed and tilted LLs for 2D Weyl materials. In general, the presence of the vector potential $\mathbf{A}^{(g)}$ in Eq. (2) breaks translational symmetry, rendering the Bloch theorem and the corresponding tight-binding approximation invalid. To overcome this problem, one possible solution, viable for both free space and lattice geometries and presented in many textbooks on quantum mechanics (see, for example,

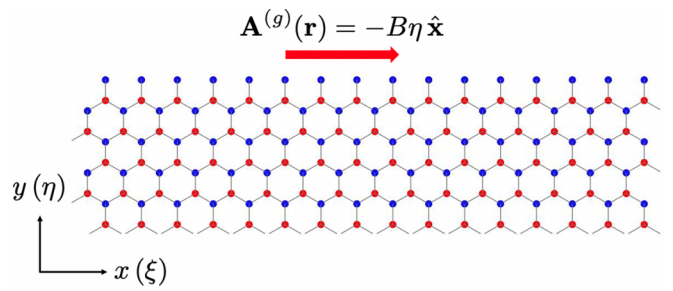


FIG. 1. Schematic representation of the geometry for a 2D Weyl material. The flake is assumed to be infinitely extended along the x direction, so that translational symmetry is unbroken along it. The gauge potential $\mathbf{A}^{(g)}$, giving rise to the out-of-plane magnetic field, is oriented along the x direction, so that its magnitude can be proportional to y , thus allowing us to decouple Landau quantization from the calculation of the effective band structure. The plot shows a regular honeycomb lattice, where the two different colors (blue and red) of the lattice sites represent the different atomic species characterizing Weyl materials. Both unscaled ($\{x, y\}$) and scaled ($\{\xi, \eta\}$) reference frames are shown for convenience.

Ref. [34] for a detailed discussion) and graphene physics [2,35,36], is to choose a preferential direction for the vector potential along which translation invariance is broken and assume translation invariance in the other direction. For the case of lattice systems such as the one depicted in Fig. 1, we choose y to be the direction of broken symmetry, so that k_x is still a good quantum number, as translational invariance is not broken along the x direction, and although we can no longer formally apply Bloch's theorem to the whole 2D material, we can still calculate an effective band structure along the x direction, which will be parametric in the y coordinate [35]. If, moreover, we choose the gauge potential $\mathbf{A}^{(g)}$ in such a way that $\mathbf{A}^{(g)} \propto y$, we can apply standard Landau quantization without breaking translational symmetry in the x direction.

The Hamiltonian above can be split into two contributions, one containing only the magnetic field through the magnetic momentum π_μ and one containing only information about the tilt through the parameters $a_{x,y}$. Before doing that, however, since in general $v_x \neq v_y$, it is first convenient to rescale both the momentum and the gauge fields \mathbf{A} and $\mathbf{A}^{(g)}$ by introducing the effective Fermi velocity $v = \sqrt{v_x v_y}$ and, consequently, the scaled momentum coordinates $k_\xi = \sqrt{v_x/v_y} k_x$ and $k_\eta = \sqrt{v_y/v_x} k_y$ and the corresponding scaled gauge field components $A_\xi = \sqrt{v_x/v_y} A_x$ and $A_\eta = \sqrt{v_y/v_x} A_y$, so that the following transformation between magnetic momenta holds:

$$v_x \pi_x \pm i v_y \pi_y \rightarrow v (\pi_\xi \pm i \pi_\eta), \quad (3)$$

meaning that then, the components of the magnetic momentum in the scaled frame are given by $\pi_\xi = \sqrt{v_x/v_y} \pi_x$ and $\pi_\eta = \sqrt{v_y/v_x} \pi_y$.

After doing this, we can then rewrite the Hamiltonian in Eq. (1) as $\hat{H} \equiv \hat{H}_0 + \hat{H}_{\text{tilt}}$, where \hat{H}_0 depends on only the gauge fields (in particular, on the applied magnetic field) and not on the tilting parameters, and its explicit expression is

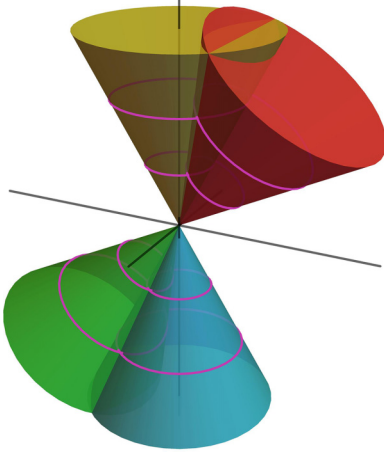


FIG. 2. Pictorial representation of untitled vs titled cones in 2D Weyl materials. The blue and orange cones represent the valence and conduction bands, respectively, of an untitled system [$\mathbf{a} = 0$ in Eq. (1)], while the green and red cones depict tilt-induced perturbation of the band structure in the vicinity of the Dirac point. The purple lines on each cone represent the LL appearing in that band due to the magnetic field.

given by

$$\hat{H}_0 = v \left[\sum_{i=1}^2 \pi_i \hat{\sigma}_i + \frac{\Delta}{v} \hat{\sigma}_3 \right] + \frac{ev}{c} \sum_{i=1}^2 A_i \hat{\sigma}_i. \quad (4)$$

The tilt Hamiltonian, on the other hand, contains the dependence on the tilting parameter $\tau_k = a_k/v_k$ and reads

$$\hat{H}_{\text{tilt}} = \sum_{i=1}^2 \left[\tau_i \left(\pi_i + \frac{e}{c} A_i \right) \right] \hat{\sigma}_i, \quad (5)$$

where now the convention $1 \rightarrow \xi$ and $2 \rightarrow \eta$ has been implicitly assumed and $\tau_{\xi,\eta} \equiv \tau_{x,y}$.

A pictorial representation of the band structure of 2D Weyl materials in the vicinity of one of their Dirac points is given in Fig. 2. In particular, the band structure given by the Hamiltonian \hat{H}_0 in Eq. (4) imposes Landau levels on a straight Dirac cone (orange and blue cones in Fig. 2), while the inclusion of the tilting Hamiltonian in Eq. (5) tilts the whole structure, i.e., Dirac cone plus Landau levels (green and red cones in Fig. 2).

III. LANDAU QUANTIZATION OF TILTED CONES

In this section we shall see how to perform the LQ for the Hamiltonian (1). To do that, we will adopt a perturbative approach, in which we first quantize \hat{H}_0 , which will give rise to the usual LLs, and then include the tilting perturbatively by promoting τ_x and τ_y to perturbative parameters. As a result of this operation, we will show how the tilting de facto introduces new transition matrix elements between the valence and conduction band LLs.

A. Standard Landau quantization

To start with, let us first consider \hat{H}_0 and solve the eigenvalue problem

$$\hat{H}_0 |\phi_n\rangle = E_n |\phi_n\rangle \quad (6)$$

in the presence of a constant magnetic field. According to Fig. 1, we can exploit translational symmetry along the x direction to write the eigenstate $|\phi_n\rangle$ as

$$|\phi_n\rangle = \int dk_\xi e^{ik_\xi \xi} |\psi_n(\eta; k_\xi)\rangle, \quad (7)$$

where $|\psi_n(k_\xi; \eta)\rangle \equiv |\psi_n\rangle$ emphasizes that the eigenstate $|\psi_n\rangle$ is function of the momentum k_ξ and depends parametrically on η . Note, moreover, that even in the absence of a magnetic field, i.e., for $\mathbf{A}^{(g)} = 0$, the above ansatz is still valid and allows for the calculation of an effective band structure, which will depend parametrically on η .

As described above, the magnetic field is inserted through minimal coupling by the substitution $\mathbf{k} \rightarrow \boldsymbol{\pi} = \mathbf{k} + \frac{e}{c} \mathbf{A}^{(g)}$, where $\mathbf{A}^{(g)}$ is the vector potential corresponding to the applied magnetic field. To make calculations easier, we can assume that we are working in the Landau gauge, where the vector potential can be chosen as

$$\mathbf{A}^{(g)} = -B\eta \hat{\mathbf{x}}. \quad (8)$$

Note that at this level of analysis, we do not make any assumption about the nature of the magnetic field. It could be an actual external magnetic field, or it could emerge as a consequence of bending or straining the material lattice, as detailed in Ref. [33]. Our formalism and calculations are insensitive to the physical origin of the magnetic field, and for this reason we will not specify one.

The easiest way to solve the above eigenvalue problem (6) is to transform \hat{H}_0 in terms of creation and annihilation operators of the harmonic oscillator. To do that, let us first observe that $[\pi_\xi, \pi_\eta] = -i(\frac{eB}{c})$ [34]. This suggests taking $q_\xi = (c/eB)\pi_\eta$ as a viable canonically conjugated generalized coordinate to the generalized momentum π_ξ . This means that π_ξ and π_η are canonically conjugated variables, and we can therefore associate creation and annihilation operators with them, as per standard quantum mechanics [37], i.e.,

$$\pi_\xi = \frac{1}{\sqrt{2}L_B} (\hat{a}^\dagger - \hat{a}), \quad (9a)$$

$$\pi_\eta = \frac{i}{\sqrt{2}L_B} (\hat{a}^\dagger + \hat{a}), \quad (9b)$$

where $[\hat{a}, \hat{a}^\dagger] = 1$ and $L_B = \sqrt{\hbar/eB}$ is the characteristic magnetic length. Substituting this into the scaled \hat{H}_0 and introducing the quantities $\lambda \equiv \Delta L_B / \sqrt{2}v$ and $\omega_c = \sqrt{2}v/L_B$, we have

$$\hat{H}_0 = \omega_c \begin{pmatrix} \lambda & \hat{a}^\dagger \\ \hat{a} & -\lambda \end{pmatrix}. \quad (10)$$

The eigenvalues and eigenstates of the Hamiltonian in Eq. (14) can then readily be calculated by substituting its expression into Eq. (6), so that the eigenvalue spectrum is finally given by

$$\varepsilon_n = s_n \sqrt{\lambda^2 + |n|}, \quad (11)$$

where $|n|$ accounts for the Landau level and $s_n = \text{sgn}(n) \equiv \pm$ accounts for valence ($-$) and conduction ($+$) bands. The (normalized) Landau spinor corresponding to the eigenstates

of \hat{H}_0 then reads

$$|\psi_n\rangle = \frac{1}{\sqrt{1 + \gamma_n^2}} \begin{pmatrix} \phi_{|n|} \\ \gamma_n \phi_{|n|-1} \end{pmatrix}, \quad (12)$$

where $\gamma_n = (\varepsilon_n - \lambda)/\sqrt{|n|}$, $\phi_n(x)$ is a harmonic oscillator eigenstate (Hermitian-Gaussian functions in one dimension) [34], and the prescription that $\phi_{-1} = 0$ is enforced. Note, moreover, that for $n = 0$ we have

$$\varepsilon_0 = \lambda, \quad (13a)$$

$$|\psi_0\rangle = \begin{pmatrix} \phi_0 \\ 0 \end{pmatrix} \quad (13b)$$

and that we need to exclude the eigenvalue $\varepsilon_0^- = -\lambda$ because for this case $\gamma_0^- \rightarrow \infty$ and therefore $|\psi_0^-\rangle \rightarrow 0$.

B. Introducing the tilting

We now consider the effect of the tilt on both Landau levels and eigenstates. We first rewrite \hat{H}_{tilt} in terms of creation and annihilation operators, following the prescription above, to obtain

$$\hat{H}_{\text{tilt}} = \omega_c [\tau_x (\hat{a}^\dagger - \hat{a}) + i\tau_y (\hat{a}^\dagger + \hat{a})] \mathbb{I}, \quad (14)$$

where $\tau_i \equiv a_i/2v_i$ is the tilting in the i direction and constitutes our perturbation parameter. To calculate the effect of the tilting on the Landau levels and eigenstates of \hat{H} in Eq. (1), we employ first-order perturbation theory using τ as the perturbation parameter. Without loss of generality, we can assume that the tilt happens only along the x direction so that $\tau_y = 0$ and $\tau \equiv \tau_x$ and the calculations are easier. This assumption essentially means that we consider a situation in which the vector potential (generating the external out-of-plane magnetic field) is aligned with the tilting direction. A more general solution with the vector potential and tilting misaligned is readily obtained by employing perturbation theory with two perturbative parameters $\tau_{x,y}$ or by simply applying a rotation operator to both the vector potential and the eigenstates of \hat{H}_0 , but it is out of the scope of this paper.

First, we expand the eigenstates and eigenvalues of the tilted system in terms of the perturbative parameter τ up to order $O(\tau^2)$, i.e., $|\psi_n\rangle = |\psi_n^{(0)}\rangle + \tau |\psi_n^{(1)}\rangle + O(\tau^2)$ and $\varepsilon_n = \varepsilon_n^{(0)} + \tau \varepsilon_n^{(1)} + O(\tau^2)$, and solve the complete eigenvalue problem up to the same order, thus obtaining

$$\begin{aligned} (\hat{H}_0 + \tau \hat{V})(|\psi_n^{(0)}\rangle + \tau |\psi_n^{(1)}\rangle) \\ = (\varepsilon_n^{(0)} + \tau \varepsilon_n^{(1)})(|\psi_n^{(0)}\rangle + \tau |\psi_n^{(1)}\rangle), \end{aligned} \quad (15a)$$

where $\hat{V} \equiv \hat{H}_{\text{tilt}}/(\tau\omega_c)$. The zero-order solution is given above (and corresponds to the untilted cones). At first order in τ we have instead

$$\hat{H}_0 |\psi_n^{(1)}\rangle + \hat{V} |\psi_n^{(0)}\rangle = \varepsilon_n^{(0)} |\psi_n^{(1)}\rangle + \varepsilon_n^{(1)} |\psi_n^{(0)}\rangle. \quad (16)$$

Note, moreover, that the normalization condition of $|\psi_n\rangle$ imposes that $\langle \psi_n^{(0)} | \psi_n^{(1)} \rangle = 0$. With this information, we can then calculate the correction to the eigenvalues by projecting Eq. (24) onto $\langle \psi_n^{(0)} |$, obtaining

$$\varepsilon_n^{(1)} = \langle \psi_n^{(0)} | \hat{V} | \psi_n^{(0)} \rangle. \quad (17)$$

It is not hard to show that $\varepsilon_n^{(1)} = 0$. Substituting this result into Eq. (24) and applying standard methods of perturbation theory, we get

$$|\psi_n^{(1)}\rangle = \sum_{m \neq n} \frac{\langle \psi_m^{(0)} | \hat{V} | \psi_n^{(0)} \rangle}{\varepsilon_n^{(0)} - \varepsilon_m^{(0)}} |\psi_m^{(0)}\rangle. \quad (18)$$

Using the (normalized) expression of \hat{V} through \hat{H}_{tilt} and the expressions of the untilted eigenstates, we get

$$\langle \psi_m^{(0)} | \hat{V} | \psi_n^{(0)} \rangle = \alpha_{n,n+1} \delta_{m,n+1} - \alpha_{n,n-1} \delta_{m,n-1}, \quad (19)$$

where

$$\alpha_{n,n+1} = \frac{\sqrt{|n|+1} + \gamma_n \gamma_{n+1} \sqrt{|n|}}{\sqrt{(1 + \gamma_n^2)(1 + \gamma_{n+1}^2)}}, \quad (20a)$$

$$\alpha_{n,n-1} = \frac{\sqrt{|n|} + \gamma_n \gamma_{n-1} \sqrt{|n|-1}}{\sqrt{(1 + \gamma_n^2)(1 + \gamma_{n-1}^2)}}. \quad (20b)$$

Substituting this result into Eq. (18), we get the following form for the perturbed eigenstates:

$$|\psi_n^{(1)}\rangle = N \begin{pmatrix} A_{n,n+1} \phi_{|n|+1} + A_{n,n-1} \phi_{|n|-1} \\ \gamma_{n+1} A_{n,n+1} \phi_{|n|} + \gamma_{n-1} A_{n,n-1} \phi_{|n|-2} \end{pmatrix}, \quad (21)$$

with $N = 1/\sqrt{1 + \gamma_n^2}$ and

$$A_{n,n\pm 1} = \frac{\sqrt{1 + \gamma_n^2}}{\varepsilon_n^{(0)} - \varepsilon_{n\pm 1}^{(0)}} \alpha_{n,n\pm 1}. \quad (22)$$

This is the first result of our work. At first order in perturbation theory, the tilting affects only the eigenstates $|\psi_n\rangle$ and not the energies of the LLs. Since, as can be seen in the equation above, the perturbative correction to the Landau eigenstates contains terms proportional to $\phi_{|n|\pm 1}$ and $\phi_{|n|-2}$, the expected impact of this perturbation in the interaction of tilted cones with an impinging electromagnetic pulse would be to modify the selection rules for the allowed transitions, thus inserting more excitation and decay channels than in the untilted case.

IV. COUPLED MODE EQUATIONS FOR THE INTERACTION HAMILTONIAN

In this section, we consider the action of an impinging, pulsed electromagnetic field and study its interaction with a system presenting tilted cones, i.e., a Weyl material. We continue working within the minimal coupling framework and simply add a second gauge field to the picture, this time representing the external pulse impinging on the Weyl material, by employing the substitution $\boldsymbol{\pi} \rightarrow \mathbf{p} = \boldsymbol{\pi} + (e/c)\mathbf{A}(t)$. The interaction Hamiltonian, comprising, as can be seen from Eqs. (4) and (5), both tilt-independent and tilt-dependent terms, then reads

$$\hat{H}_{\text{light}} = \frac{ev}{c} \left[\sum_{i=1}^2 A_i \hat{\sigma}_i + 2\tau (A_\xi + iA_\eta) \mathbb{I} \right]. \quad (23)$$

Without loss of generality, we can assume the impinging optical pulse is polarized along the ξ direction (i.e., along the x

direction), so that we can set $A_\eta = 0$ and write

$$A_\xi \equiv A(t) = E_0 \tau e^{-\frac{(t-t_0)^2}{\Delta t^2}} \cos(\omega_L t), \quad (24)$$

where E_0 is the amplitude of the impinging electric field, Δt is the pulse duration, and ω_L is the pulse central frequency. Note that since in the previous section we assumed the Dirac cone is tilted along the x direction (i.e., we set $\tau_y = 0$), the assumption made above essentially corresponds to the case in which the impinging field is polarized along the tilting direction.

With the light-matter Hamiltonian in hand, we can then cast the time-dependent Dirac equation in the following form:

$$i \frac{\partial}{\partial t} |\Psi(t)\rangle = [\hat{H}_0 + \hat{H}_{\text{tilt}} + \hat{H}_{\text{light}}(t)] |\Psi(t)\rangle. \quad (25)$$

To solve it, we expand the real solution in the instantaneous eigenstates calculated above, i.e.,

$$|\Psi(t)\rangle = \sum_n [c_n^+(t) e^{-i\omega_n t} |\psi_n^+\rangle + c_n^-(t) e^{i\omega_n t} |\psi_n^-\rangle], \quad (26)$$

where $|\psi_n\rangle = |\psi_n^{(0)}\rangle + \tau |\psi_n^{(1)}\rangle$, $\omega_n = |\varepsilon_n| = \sqrt{\lambda^2 + |n|}$, and $\sum_n (|c_n^+|^2 + |c_n^-|^2) = 1$. Substituting this ansatz into the equation above and remembering that $|\psi_n\rangle$ are (perturbative) eigenstates of $\hat{H}_0 + \hat{H}_{\text{tilt}}$, we get the following set of coupled mode equations for the time-dependent coefficients:

$$i \dot{c}_m^+ = \sum_n [\langle \psi_m^+ | \hat{H}_{\text{light}}(t) | \psi_n^+ \rangle e^{-i(\omega_n - \omega_m)t} c_n^+ + \langle \psi_m^+ | \hat{H}_{\text{light}}(t) | \psi_n^- \rangle e^{i(\omega_n + \omega_m)t} c_n^-], \quad (27a)$$

$$i \dot{c}_m^- = \sum_n [\langle \psi_m^- | \hat{H}_{\text{light}}(t) | \psi_n^+ \rangle e^{-i(\omega_n + \omega_m)t} c_n^+ + \langle \psi_m^- | \hat{H}_{\text{light}}(t) | \psi_n^- \rangle e^{i(\omega_n - \omega_m)t} c_n^-]. \quad (27b)$$

To solve these coupled mode equations, one first needs to write down the matrix elements $\langle \psi_m^\pm | \hat{H}_{\text{light}}(t) | \psi_n^\pm \rangle$. To do so, let us assume that the carrier frequency of the impinging pulse is resonant with the transition $|\psi_{-1}\rangle \rightarrow |\psi_0\rangle$ (corresponding to the transition between the zero-energy state and the first LL in the valence band) and then set $\omega_L = |\omega_0 - \omega_1| = \sqrt{\lambda^2 + 1} - \lambda$.

In the untilted case, selection rules allow only transitions that obey $\Delta|n| = 1$ [38], which corresponds to choosing matrix elements of the form $\langle \psi_{m,\pm}^{(0)} | \hat{H}_{\text{light}} | \psi_{n,\pm}^{(0)} \rangle \simeq \delta_{|m|,|n|+1} + \delta_{|m|,|n|-1}$.

In the presence of tilt, however, the selection rule above is not valid anymore, and new selection rules appear due to the fact that the matrix elements of the interaction Hamiltonian calculated with respect to the perturbed eigenstates read

$$\langle \psi_{m,\pm}^{(1)} | \hat{H}_{\text{light}} | \psi_{n,\pm}^{(1)} \rangle \simeq \delta_{|m|,|n|+2} + \delta_{|m|,|n|-2}. \quad (28)$$

Combining this extra set of selection rules with those of the usual, untilted case, we can write the tilt-induced selection rules as follows:

$$0 < \Delta|n| \leq 2. \quad (29)$$

This is the second result of our work. The tilt in Dirac cones introduces an extra set of selection rules for light-matter interaction, which essentially originates from the eigenstate mixing imposed by the tilt itself [see Eq. (21)]. A schematic representation of the different sets of selection rules for the

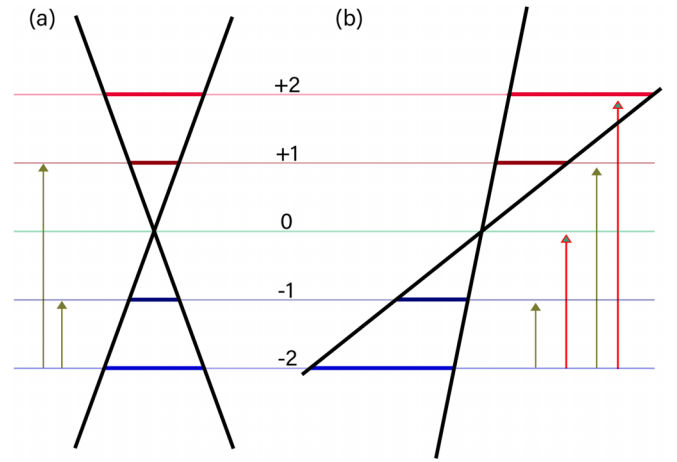


FIG. 3. Band structure of LLs in the vicinity of the Dirac points for the case of (a) untilted and (b) tilted cones. As can be seen, in (a), the selection rules dictate, for example, that only the transitions represented by gray lines, i.e., $|\psi_{-2}\rangle \rightarrow |\psi_{-1}\rangle$ and $|\psi_{-2}\rangle \rightarrow |\psi_1\rangle$, are possible (assuming that $|\psi_{-2}\rangle$ is the only initially populated level). When the cone is tilted in (b), however, the red transitions, i.e., $|\psi_{-2}\rangle \rightarrow |\psi_0\rangle$ and $|\psi_{-2}\rangle \rightarrow |\psi_2\rangle$, become allowed. This is possible due to the tilting extending the selection rules to encompass also $\Delta|n| = 2$ as a viable option. Note that in going from (a) to (b), while the valence and conduction bands are being tilted, the energy levels are not because they are, at first order in perturbation theory, unaffected by the tilting. This, ultimately, is one of the reasons for the appearance of extra selection rules.

untilted and tilted cases is shown in Fig. 3. A more careful analysis of these selection rules reveals that while the simplest model to describe light-matter interaction for untilted Dirac cones is a three-level system (see, for example, Ref. [39]), in the case of tilted cones, the simplest system that catches the essential physics of tilted cones in a magnetic field is a five-level system.

V. NONLINEAR OPTICAL RESPONSE

Once the coupled mode equations have been solved, we can proceed with calculating the current, with its usual definition, i.e.,

$$\mathbf{J}(t) = \langle \Psi(t) | \boldsymbol{\sigma} | \Psi(t) \rangle, \quad (30)$$

where $\boldsymbol{\sigma} = \sigma_x \hat{\mathbf{x}} + \sigma_y \hat{\mathbf{y}}$. Substituting the expansion (26) into the above equation, we get, for the components of the current,

$$J_\mu(t) = \sum_{n,m} [(c_m^+)^* c_n^+ e^{i(\omega_m - \omega_n)t} \langle \psi_m^+ | \sigma_\mu | \psi_n^+ \rangle + (c_m^+)^* c_n^- e^{i(\omega_m + \omega_n)t} \langle \psi_m^+ | \sigma_\mu | \psi_n^- \rangle + (c_m^-)^* c_n^+ e^{-i(\omega_m + \omega_n)t} \langle \psi_m^- | \sigma_\mu | \psi_n^+ \rangle + (c_m^-)^* c_n^- e^{-i(\omega_m - \omega_n)t} \langle \psi_m^- | \sigma_\mu | \psi_n^- \rangle], \quad (31)$$

and the expectation values of the Pauli matrices over the perturbed states can be calculated up to order $O(\tau)$ using the results from the previous section. From here, we can then calculate the Fourier transform of the induced current and the corresponding nonlinear signal as $I(\omega) \sim |\omega \mathbf{J}(\omega)|^2$, where $\mathbf{J}(\omega)$ is the Fourier transform of the nonlinear current.

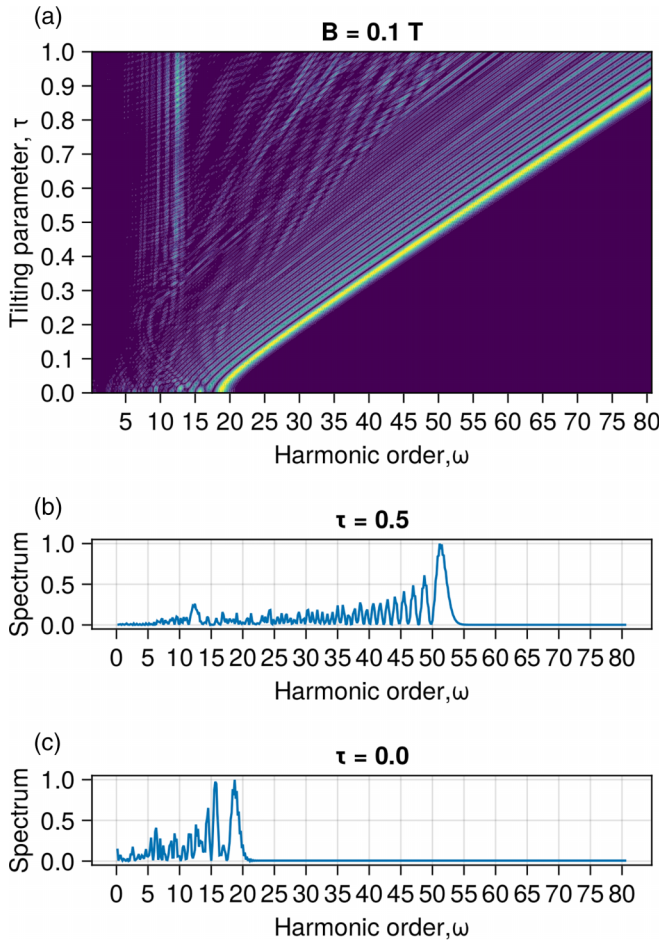


FIG. 4. (a) Spectrum for different values of the tilting parameter τ , with the magnetic field intensity set to $B = 0.1$ T. (b) and (c) The individual spectrum for $\tau = 0.5$ and $\tau = 0$, respectively. As can be seen, the tilting of a cone shifts the higher harmonic of the spectrum to higher orders, with a slope, estimated from (a), of about 72 Hz.

To study the nonlinear optical response of the system under consideration we solve coupled mode equations for the time-dependent coefficients defined by Eq. (27) using the JULIA package DIFFERENTIALEQUATIONS.JL [40], and then we

compute the nonlinear electrical current using Eq. (31) and the definition of the nonlinear signal given above. As stated at the end of the previous section, we employ a five-level model to describe the nonlinear response of 2D Weyl materials; that is, our model contains only two levels in the valence band, namely, $|\psi_{-2}\rangle$ and $|\psi_{-1}\rangle$, and two levels in the conduction band, i.e., $|\psi_1\rangle$ and $|\psi_2\rangle$. The zero-energy state $|\psi_0\rangle$, common to both Landau oscillators, constitutes the fifth level. As initial condition, we assume that only the lowest LL is occupied, i.e., $c_{-2}(0) = 1$. Moreover, we assume an impinging electromagnetic pulse with an amplitude of $E_0 = 10^7$ V/m; a carrier frequency of $\omega_L = 78$ THz, resonant with the transition $|\psi_{-2}\rangle \rightarrow |\psi_0\rangle$; and a pulse duration of $\tau = 50$ fs. We performed simulations while varying the tilting parameter for both the cases of fixed and varying magnetic field strength. The results of these simulations are depicted in Figs. 4 and 5, respectively. However, before focusing on those results, let us first concentrate on Fig. 6. There, we plot the nonlinear response of a 2D Weyl material in the presence of a weak magnetic field for the case where the impinging electric field is polarized in the direction orthogonal to that of the tilt; that is, for Fig. 6 we have assumed $A_\xi = 0$ and set A_η to be equal to Eq. (24). The parameters for this simulation, moreover, are the same as those listed above. As can be seen from Fig. 6, for the case of orthogonally polarized (with respect to the tilt direction) pulses, the only effect of the tilting is to suppress higher harmonics for values of the tilting parameter $\tau \geq 0.3$, and no particularly interesting dynamics occurs.

The situation where the impinging field is aligned with the direction of the tilt, on the other hand, is profoundly different. Let us first discuss the case of fixed magnetic field. To start with, let us use the value $B = 0.1$ T for the magnetic field. We will then investigate the influence of different values of the magnetic field amplitudes later in this section. As can be seen from Fig. 6(c), for $\tau = 0$, i.e., untilted cones, our results are consistent with those obtained in Ref. [39] [compare our Fig. 6(c), for example, with Fig. 6(a) therein], even though in our case we obtain a similar result with a magnetic field approximately one order of magnitude lower than the one used in Ref. [39]. This can be simply imputable to the presence of a nonzero gap between the valence and conduction bands in 2D Weyl materials, which is absent in graphene. As soon as we

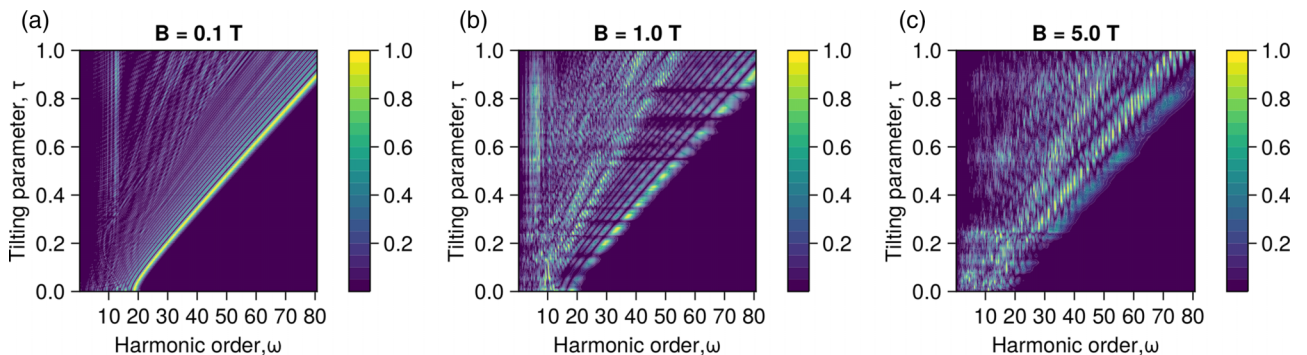


FIG. 5. Contour plots of the spectrum with the harmonic order on the x axis and tilting parameter on the y axis for different values of magnetic field amplitude: (a)–(c) 0.1, 1.0, and 5.0 T, respectively. We can see a trend on highest harmonic that a generated relative to tilting parameter, and moreover, this trend is conserved for different magnetic field amplitudes. An increase in magnetic field causes higher nonlinear effects; thus, more harmonics are generated in the nonlinear optical response.

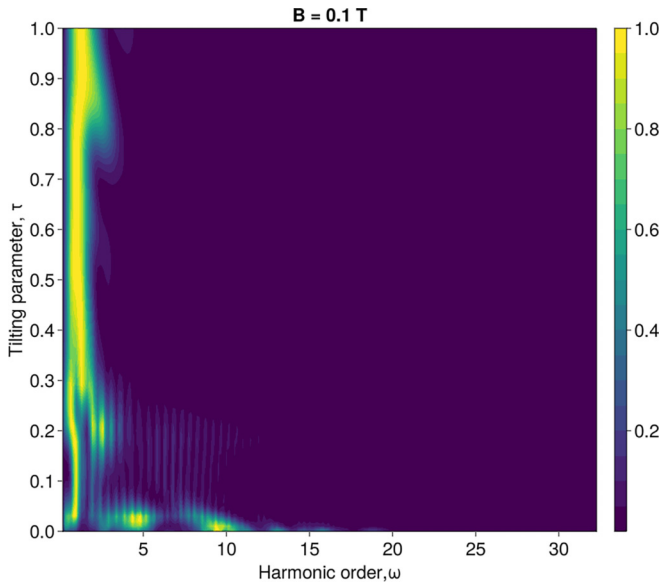


FIG. 6. Spectrum for different values of the tilting parameter τ with the magnetic field intensity set to $B = 0.1\text{T}$. The polarization of the impinging electromagnetic field in this case is orthogonal to the tilting direction; that is, the electric field is polarized along the η (y) direction. As can be seen, the only effect of the tilting in this case is to suppress harmonics higher than the fundamental ones for values of the tilting parameter $\tau \geq 0.3$.

turn on the tilt, we can see from Fig. 4(a) that an increase of the tilt parameter τ corresponds to a blueshift of the harmonic spectrum, which, in turn, allows the generation of higher harmonics than in the untilted case. Figure 4(a), moreover, shows how the blueshift of the maximum of the harmonic spectrum is approximately linear with τ . This phenomenon is a consequence of the fact that the kinetic momentum of an electron in the vicinity of a tilted cone is given by $\mathbf{p} = \mathbf{k} + (e/c)\mathbf{A}^{(g)} + (e/c)\mathbf{A}$. In this scenario, the vector potential $\mathbf{A}^{(g)}$ linearly displaces the electron momentum [see Eq. (8)]. The action of this linear displacement, combined with the action of the tilting on the interaction Hamiltonian, ultimately makes sure that the blueshift experienced by the nonlinear spectrum is linear in τ . As a concrete example of the possibility this offers for light-matter interaction engineering, in Fig. 4(b) we explicitly point to the case $\tau = 0.5$, where the maximum of the spectrum now sits around the 50th harmonic. Considering the input carrier frequency of $\omega_L = 78$ THz, its 50th harmonic corresponds to $\omega_{50} = 3900$ THz, i.e., $\lambda \simeq 480$ nm. By suitably engineering 2D Weyl materials to possess a tilt of $\tau = 0.5$ (along the x direction, in our case, but the same line of reasoning would hold for an anisotropic tilt), it would be then possible to realize a frequency converter capable of implementing efficient conversion of light between the terahertz (THz) and visible (blue, in this case) domains.

Figure 5, instead, shows how different values of the magnetic field affect the tilt-induced blueshift. As can be seen, while the shift induced by the tilting parameter τ remains essentially unaltered by an increasing amplitude of the applied magnetic field, an increase of the latter changes the nonlinear

optical response of the system. In particular, it redistributes the energy between the various harmonics, as can be seen, for example, in Fig. 5(b), where intermediate harmonics have higher intensity than the case with small magnetic field [see Fig. 5(a), for example]. Moreover, increasing the magnetic field even further leads to a more complicated scenario, as depicted in Fig. 5(c), where the nonlinear response as a function of τ becomes much more complex. However, the blueshift effect reported by our simulations is genuinely an effect of the tilting parameter τ because it persists independently of the value of the applied magnetic field, as can be seen from Fig. 5, where, despite the “noise” introduced by the higher magnetic field, the dependence of the nonlinear response on the tilting parameter τ remains the same.

VI. CONCLUSION

In this work, we have studied how tilted Dirac cones in 2D Weyl materials are affected by the presence of an external (or artificial) magnetic field. We derived the analytical expression for the LLs and eigenstates for the case of tilted cones using first-order perturbation theory and have shown that when 2D Weyl materials in the presence of magnetic field interact with electromagnetic pulses, the tilting induces an extra set of selection rules, which extends the usual ones to $0 < \Delta|n| \leq 2$. We then computed the nonlinear optical response of 2D Weyl materials immersed in magnetic fields and noticed that by controlling the tilt of their cones, it is possible to achieve a versatile and precise control of their nonlinear spectrum and that by engineering Weyl materials with greatly tilted cones, it is possible to achieve high-harmonic generation up to the 80th harmonic for $\tau \rightarrow 1$. However, accounting for a more physically feasible situation, we discussed the case of $\tau = 0.5$, where the 50th harmonic appears in the spectrum, thus enabling efficient transfer of energy between THz and UV radiation. In comparison, Ref. [39] discussed the efficient THz-to-visible conversion of radiation in graphene in the presence of a magnetic field of 2 T. Here, instead, the tilting not only can serve as a tuning parameter to enhance the generated harmonic, allowing access to different spectral regions, but also enables the same efficiency with much lower values of the magnetic field, roughly one order of magnitude lower than that used in Ref. [39].

Finally, we studied the impact of the magnetic field on this process and concluded that while the overall trend does not change, a change in the magnetic field intensity corresponds to a redistribution of energy through the harmonics in the spectrum, thus resulting in a more complex picture that could offer some degree of control over the frequency conversion process in such materials.

Our results show that by suitably engineering 2D Weyl materials to possess specific tilting properties and by controlling the applied magnetic field (for example, through strain and bending), it is possible to realize efficient THz-to-visible frequency converters or to employ such devices (in particular, their sensitivity to the magnetic field) for sensing applications, where, for example, a local change in the lattice structure (due, for example, to the adsorption of a certain molecule) could vary (via artificial gauge) the intensity of the magnetic field and therefore the response of the material.

ACKNOWLEDGMENTS

Y.T. and M.O. acknowledge the financial support from the Academy of Finland Flagship Programme, Photonics research and innovation (PREIN), Decision No. 320165. Y.T. also acknowledges support from the Finnish Cultural Foundation, Decision No. 00221008. L.D.M.V. acknowledges support from the European Commission under the EU Horizon 2020 MSCA-RISE-2019 program (Project No. 873028 HYDROTRONICS) and from the Leverhulme Trust under Grant No. RPG-2019-363.

APPENDIX: SECOND-ORDER CORRECTION TO THE LANDAU SPECTRUM

In this Appendix, we briefly present the general form of the first nonzero correction to the LLs as a function of the perturbative tilt parameter τ . As stated in the main text, it is fairly easy to show that $\varepsilon^{(1)} = 0$. Therefore, the first nonzero correction to the LL energy spectrum would be quadratic in τ . To achieve this, we need to consider also second-order contributions to Eq. (15), i.e.,

$$\begin{aligned} & (\hat{H}_0 + \tau\hat{V})(|\psi_n^{(0)}\rangle + \tau|\psi_n^{(1)}\rangle + \tau^2|\psi_n^{(2)}\rangle) \\ &= (\varepsilon_n^{(0)} + \tau\varepsilon_n^{(1)} + \tau^2\varepsilon_n^{(2)})(|\psi_n^{(0)}\rangle + \tau|\psi_n^{(1)}\rangle + \tau^2|\psi_n^{(2)}\rangle), \end{aligned} \quad (\text{A1})$$

from which the second-order correction to the energy eigenvalues $\varepsilon_n^{(2)}$ can be calculated using the first-order results discussed in Sec. III B together with the requirement that

$$2\langle\psi_n^{(0)}|\psi_n^{(2)}\rangle + \langle\psi_n^{(1)}|\psi_n^{(1)}\rangle = 0 \quad (\text{A2})$$

to obtain the following expression for the second-order correction to the energy (the interested reader can check out the whole calculation in any standard quantum mechanics textbook, for example, Ref. [37]):

$$\varepsilon_n^{(2)} = \sum_{m \neq n} \frac{|\langle\psi_m^{(0)}|\hat{V}|\psi_n^{(0)}\rangle|^2}{\varepsilon_n^{(0)} - \varepsilon_m^{(0)}}, \quad (\text{A3})$$

where, as before, $\hat{V} = \hat{H}_{\text{tilt}}/\tau$ and \hat{H}_{tilt} is given by Eq. (14). To calculate the argument of the modulus square of the numerator, we can use Eq. (19) to get

$$\begin{aligned} |\langle\psi_m^{(0)}|\hat{V}|\psi_n^{(0)}\rangle|^2 &= |\alpha_{n,n+1}\delta_{m,n+1} - \alpha_{n,n-1}\delta_{m,n-1}|^2 \\ &= |\alpha_{n,n+1}|^2\delta_{m,n+1} + |\alpha_{n,n-1}|^2\delta_{m,n-1}. \end{aligned} \quad (\text{A4})$$

Note that in going from the first to the second line of the expression above, we have used the fact that the mixed term coming from the modulus square is proportional to $\delta_{m,n+1}\delta_{m,n-1} = \delta_{n-1,n+1} = 0$ and therefore can be neglected. Using the result above, we can then write the second-order correction as follows:

$$\varepsilon_n^{(2)} = \frac{|\alpha_{n,n+1}|^2}{\varepsilon_n^{(0)} - \varepsilon_{n+1}^{(0)}} + \frac{|\alpha_{n,n-1}|^2}{\varepsilon_n^{(0)} - \varepsilon_{n-1}^{(0)}}. \quad (\text{A5})$$

We leave to the reader the rather cumbersome task of finding the explicit expression of $\varepsilon_n^{(2)}$ as an explicit function of the index n and the energy scale λ . Per se, this task is not particularly difficult; one, in fact, only needs to substitute in the expression above the explicit expressions for the coefficients $\alpha_{n,n \pm 1}$ given by Eqs. (20) and the expression for $\varepsilon_m^{(0)}$ given by Eq. (11). The resulting expression is quite complicated and cannot easily be simplified to a nice and compact form.

Finally, we can then write the explicit form of the dependence of the Landau energies on the tilting parameter τ as the following second-order-accurate form:

$$\varepsilon_n = s_n\sqrt{\lambda^2 + |n|} + \tau^2 \frac{B_n}{[\varepsilon_n^{(0)} - \varepsilon_{n+1}^{(0)}][\varepsilon_n^{(0)} - \varepsilon_{n-1}^{(0)}]}, \quad (\text{A6})$$

where

$$B_n = |\alpha_{n,n+1}|^2[\varepsilon_n^{(0)} - \varepsilon_{n-1}^{(0)}] + |\alpha_{n,n-1}|^2[\varepsilon_n^{(0)} - \varepsilon_{n+1}^{(0)}]. \quad (\text{A7})$$

-
- [1] K. S. Novoselov, A. K. Geim, S. V. Morozov, Y. Z. D. Jiang, S. V. Dubonos, I. V. Grigorieva, and A. A. Firsov, Electric field effect in atomically thin carbon films, *Science* **306**, 666 (2004).
- [2] A. H. Castro Neto, F. Guinea, N. M. R. Peres, K. S. Novoselov, and A. K. Geim, The electronic properties of graphene, *Rev. Mod. Phys.* **81**, 109 (2009).
- [3] Y. Zhang, Y.-W. Tan, H. L. Stormer, and P. Kim, Experimental observation of the quantum Hall effect and Berry's phase in graphene, *Nature (London)* **438**, 201 (2005).
- [4] L. Landau, Diamagnetismus der metalle, *Z. Phys.* **64**, 629 (1930).
- [5] W. J. de Haas and P. M. van Alphen, The dependence of the susceptibility of diamagnetic metals upon the field, *Leiden Commun. A* **212**, 215 (1930); *Proc. R. Acad. Sci. Amsterdam* **33**, 1106 (1930).
- [6] L. Schubnikow and W. D. Haas, Magnetic resistance increase in single crystals of bismuth at low temperatures, *Proc. R. Neth. Acad. Arts Sci.* **33**, 130 (1930).
- [7] L. Schubnikow and W. D. Haas, New phenomena in the change in resistance of bismuth crystals in a magnetic field at the temperature of liquid hydrogen (i), *Proc. R. Neth. Acad. Arts Sci.* **33**, 363 (1930).
- [8] M. O. Goerbig, J.-N. Fuchs, G. Montambaux, and F. Piéchon, Tilted anisotropic Dirac cones in quinoid-type graphene and α -(BEDT-TTF)₂I₃, *Phys. Rev. B* **78**, 045415 (2008).
- [9] M. O. Goerbig, J.-N. Fuchs, G. Montambaux, and F. Piéchon, Electric-field-induced lifting of the valley degeneracy in α -(BEDT-TTF)₂I₃ Dirac-like Landau levels, *Europhys. Lett.* **85**, 57005 (2009).
- [10] J. Sári, M. O. Goerbig, and C. Tóke, Magneto-optics of quasirelativistic electrons in graphene with an inplane electric field and in tilted Dirac cones in α -(BEDT TTF)₂I₃, *Phys. Rev. B* **92**, 035306 (2015).
- [11] J. Wyzula, X. Lu, D. Santos-Cottin, D. K. Mukherjee, I. Mohelský, F. Le Mardelé, J. Novák, M. Novak, R. Sankar, Y. Krupko, B. A. Piot, W.-L. Lee, A. Akrap, M. Potemski,

- M. O. Goerbig, and M. Orlita, Lorentz-boost-driven magneto-optics in a Dirac nodal-line semimetal, *Adv. Sci.* **9**, 2105720 (2022).
- [12] S. Tchoumakov, M. Civelli, and M. O. Goerbig, Magnetic-Field-Induced Relativistic Properties in Type-I and Type-II Weyl Semimetals, *Phys. Rev. Lett.* **117**, 086402 (2016).
- [13] A. A. Soluyanov, D. Gresch, Z. Wang, Q. Wu, M. Troyer, X. Dai, and B. Andrei Bernevig, Type-II Weyl semimetals, *Nature (London)* **527**, 495 (2015).
- [14] M. Yan, H. Huang, K. Zhang, E. Wang, W. Yao, K. Deng, G. Wan, H. Zhang, M. Arita, H. Yang, Z. Sun, H. Yao, Y. Wu, S. Fan, W. Duan, and S. Zhou, Lorentz-violating type-II Dirac fermions in transition metal dichalcogenide PtTe₂, *Nat. Commun.* **8**, 257 (2017).
- [15] L. L. Tao and E. Y. Tsymbal, Two-dimensional type-II Dirac fermions in a LaAlO₃/LaNiO₃/LaAlO₃ quantum well, *Phys. Rev. B* **98**, 121102(R) (2018).
- [16] H. J. Noh, J. Jeong, E. J. Cho, K. Kim, B. I. Min, and B. G. Park, Experimental Realization of Type-II Dirac Fermions in a PdTe₂ Superconductor, *Phys. Rev. Lett.* **119**, 016401 (2017).
- [17] Y. Xu, F. Zhang, and C. Zhang, Structured Weyl Points in Spin-Orbit Coupled Fermionic Superfluids, *Phys. Rev. Lett.* **115**, 265304 (2015).
- [18] K. Koepnick, D. Kasinathan, D. V. Efremov, S. Khim, S. Borisenko, B. Büchner, and J. van den Brink, TaIrTe₄: A ternary type-II Weyl semimetal, *Phys. Rev. B* **93**, 201101(R) (2016).
- [19] T. E. O'Brien, M. Diez, and C. W. J. Beenakker, Magnetic Breakdown and Klein Tunneling in a Type-II Weyl Semimetal, *Phys. Rev. Lett.* **116**, 236401 (2016).
- [20] G. Autès, D. Gresch, M. Troyer, A. A. Soluyanov, and O. V. Yazyev, Robust Type-II Weyl Semimetal Phase in Transition Metal Diphosphides XP₂ (X = Mo, W), *Phys. Rev. Lett.* **117**, 066402 (2016).
- [21] J. Ma, Q. Gu, Y. Liu, J. Lai, P. Yu, X. Zhuo, Z. Liu, J.-H. Chen, J. Feng, and D. Sun, Nonlinear photoresponse of type-II Weyl semimetals, *Nat. Mater.* **18**, 476 (2019).
- [22] Y.-Y. Lv, J. Xu, S. Han, C. Zhang, Y. Han, J. Zhou, S.-H. Yao, X.-P. Liu, M.-H. Lu, H. Weng, Z. Xie, Y. B. Chen, J. Hu, Y.-F. Chen, and S. Zhu, High-harmonic generation in Weyl semimetal β -wp₂ crystals, *Nat. Commun.* **12**, 6437 (2021).
- [23] Y. Tamashevich, L. D. M. Villari, and M. Ornigotti, Nonlinear optical response of type-II Weyl fermions in two dimensions, *Phys. Rev. B* **105**, 195102 (2022).
- [24] Z. Lan, N. Goldman, A. Bermudez, W. Lu, and P. Öhberg, Dirac-Weyl fermions with arbitrary spin in two-dimensional optical superlattices, *Phys. Rev. B* **84**, 165115 (2011).
- [25] T. He, X. Zhang, Y. Liu, X. Dai, G. Liu, Z.-M. Yu, and Y. Yao, Ferromagnetic hybrid nodal loop and switchable type-I and type-II Weyl fermions in two dimensions, *Phys. Rev. B* **102**, 075133 (2020).
- [26] H. Isobe and N. Nagaosa, Coulomb Interaction Effect in Weyl Fermions with Tilted Energy Dispersion in Two Dimensions, *Phys. Rev. Lett.* **116**, 116803 (2016).
- [27] Y. Guo, Z. Lin, J. Q. Zhao, J. Lou, and Y. Chen, Two-dimensional tunable Dirac/Weyl semimetal in non-Abelian gauge field, *Sci. Rep.* **9**, 18516 (2019).
- [28] J.-Y. You, C. Chen, Z. Zhang, X.-L. Sheng, S. A. Yang, and G. Su, Two-dimensional Weyl half-semimetal and tunable quantum anomalous Hall effect, *Phys. Rev. B* **100**, 064408 (2019).
- [29] Q. Lin, M. Xiao, L. Yuan, and S. Fan, Photonic Weyl point in a two-dimensional resonator lattice with a synthetic frequency dimension, *Nat. Commun.* **7**, 13731 (2016).
- [30] K. Bender, I. Hennig, D. Schweitzer, K. Dietz, H. Endres, and H. J. Keller, Synthesis, structure and physical properties of a two-dimensional organic metal, di[bis(ethylenedithiolo)tetrathiofulvalene] triiodide, α -(BEDT-TTF)₂I₃, *Mol. Cryst. Liq. Cryst.* **108**, 359 (1984).
- [31] H. Kino and T. Miyazaki, First-principles study of electronic structure in α -(BEDT-TTF)₂I₃ at ambient pressure and with uniaxial strain, *J. Phys. Soc. Jpn.* **75**, 034704 (2006).
- [32] N. Tajima and K. Kajita, Experimental study of organic zero-gap conductor α -(BEDT-TTF)₂I₃, *Sci. Technol. Adv. Mater.* **10**, 024308 (2009).
- [33] M. Vozmediano, M. Katsnelson, and F. Guinea, Gauge fields in graphene, *Phys. Rep.* **496**, 109 (2010).
- [34] L. D. Landau and E. M. Lifshitz, *Quantum Mechanics: Non-relativistic Theory* (Butterworth-Heinemann, Oxford, England, 1981).
- [35] M. I. Katsnelson, *Graphene: Carbon in Two Dimensions* (Cambridge University Press, Cambridge, 2012).
- [36] M. O. Goerbig, Electronic properties of graphene in a strong magnetic field, *Rev. Mod. Phys.* **83**, 1193 (2011).
- [37] A. Messiah, *Quantum Mechanics* (Dover, Mineola, NY, 2014).
- [38] D. S. L. Abergel and V. I. Fal'ko, Optical and magneto-optical far-infrared properties of bilayer graphene, *Phys. Rev. B* **75**, 155430 (2007).
- [39] M. Ornigotti, L. Ornigotti, and F. Biancalana, Generation of half-integer harmonics and efficient THz-to-visible frequency conversion in strained graphene, *APL Photon.* **6**, 060801 (2021).
- [40] C. Rackauckas and Q. Nie, Differentialequations.jl—A performant and feature-rich ecosystem for solving differential equations in julia, *J. Open Res. Software* **5**, 15 (2017).